Journal of Southeast University (English Edition) Vol. 25, No. 1, pp. 52 – 56 Mar. 2009 ISSN 1003—7985

Nonlinear dynamical response of high-voltage transmission lines based on cable dropping

Xia Kaiquan[1] Liu Yun[2] Qian Zhendong[2]

([1]China Electric Power Research Institute, Beijing 100055, China)

([2]Intelligent Transportation System Research Center, Southeast University, Nanjing 210096, China)

Abstract: In order to study the dynamic response of high-voltage transmission lines under mechanical failure, a finite element model of a domestic 500-kV high-voltage transmission line system is established. The initial equilibrium condition of the coupling system model is verified by nonlinear static analysis. The transient dynamic analysis method is proposed to analyze the variation law of dynamic response under cable or insulator rupture, and the dynamic response of structural elements next to the broken span is calculated. The results show that upper crossarm cable rupture has no effect on cable tension at adjacent suspension points, but it has a significant influence on tension in the insulator and the tower component of the upper crossarm next to the broken span. The peak tension in the conductor of the upper crossarm at the suspension point exceeds the design value under insulator rupture. Insulator rupture has no effect on the tower component of the upper crossarm, but it has a significant influence on insulator tension of the upper crossarm. Insulator rupture should be taken into account in the design of overhead transmission lines. The research results can provide a theoretical basis for the design of transmission lines.

Key words: high-voltage transmission line; transient response; cable dropping; numerical simulation; finite element method

Overhead transmission lines are frequently threatened by environmental loads such as wind and ice. Besides electrical technical support, mechanical reliability and safety are required. In the technical code for designing 110 to 500 kV overhead transmission lines in China[1–2], the shock loads induced by cable rupture are considered in tower design, and most calculations are based on static load cases. A transmission line system would be subjected to accidental loads such as shock loads induced by conductor or insulator rupture. Under certain circumstances, the dynamic effects also need to be examined. The occurrence of sudden rupture of cables or insulators is rare and unpredictable, and the amplitude of the forces generated is significant.

The use of computer software to study cable ruptures began in the 1980s. The first models of Siddiqui[3] were attempts to evaluate the peak longitudinal loads generated by a breakage using energy balance principles. The work of Baenziger et al. [4–5] included finite element modeling of the cables in two dimensions and some simplified tower modeling. By varying line parameters, these studies have further contributed to the understanding of the peak transient response of a line section to conductor ruptures. McClure et al. [6–7] studied the complete dynamic interaction among all line components by using a general finite element method. There are other noteworthy contributions[8–10] to the study of dynamic response monitoring, which are based on some field instrumentation and testing programmes.

1 Calculation Hypothesis and Modeling Approach

Numerical methods based on finite element analysis have the advantage of being applicable to specific line sections with variable degrees of details. The proposed numerical model is based on the application of the displacement-based finite element method to large kinematics.

1.1 Cable modeling

Conductors are represented by two-node isoperimetric truss elements with three translational degrees-of-freedom available at each node in a three-dimensional model. The cable elements are modeled by using a tension-only linear elastic material so that cable slackness can be achieved in the dynamic simulations. To ensure that the initial stiffness matrix of the system is nonsingular, a constant initial prestrain that represents the installation conditions is prescribed as an initial condition for all cable elements. This initial strain is obtained for each element of a specific span from a preliminary static analysis assuming an axially rigid catenary under gravity loads. The same catenary profile also serves to define the initial geometry of the cable profile. Small strains are assumed, and large displacement kinematics is considered in a total Lagrangian formulation.

Structural damping of the cable is modelled with equivalent viscous damping by using a lumped parameter model. In this model, each node is assigned a viscous damping constant which is independent in the horizontal and vertical directions. The values of the viscous damping constants selected in this problem[7] are based on 2% of critical damping for the bare cable.

1.2 Insulator modeling

Suspension insulator strings are modeled by using a single two-node isoperimetric truss element without initial strain, and it is supposed to be pinned to the tower at the top and to the suspended cable. It is allowed to swing freely in its own plane if there is any unbalanced load on either side of the adjacent spans. However, the catenary configuration of the insulator string due to its own weight is negligible.

Insulator strings are assumed to be made of linear elastic material with a large axial rigidity. The damping of the insulator string is not modelled as its effects should be small compared with those of cable damping in the whole system.

Received 2008-05-19.

Biography: Xia Kaiquan (1969—), male, doctor, senior engineer, xiakq@epri.ac.cn.

Foundation items: The National Natural Science Foundation of China (No. 50578038), the Science and Technology Project of the State Grid Corporation of China (No. SGKJ [2007]116).

Citation: Xia Kaiquan, Liu Yun, Qian Zhendong. Nonlinear dynamical response of high-voltage transmission lines based on cable dropping[J]. Journal of Southeast University (English Edition), 2009, 25(1): 52 – 56.

1.3 Tower modeling

Towers are represented as spatial frame structures. The torsional and flexural rigidities of the supports are included. The detailed tower models have the linear elastic material properties of structural steel when strain rate effects are ignored. The towers are assumed to be fixed on rigid foundations. Dead-end structures are represented by fixed points. Since the transient response near the cable attachment points at the supports is a main focus of the analysis, no damping is considered in the tower models.

The transmission tower is a space pole structure. If all the tower members are simulated by general truss elements, it leads to tower structure instability. The chord and main web members are modeled by spatial beam elements, and the secondary members are modeled by truss elements. The damping ratio of the tower members is 0.01[11]. The nonlinear Rayleigh damping is adopted in the whole structure of a line section.

2 Dynamic Analysis Method

If the conductor or insulator breaks, the conductor becomes a geometrical variable system. The conductor moves under gravity action, and the complicated transient dynamic response propagates in structural members due to the tower-conductor coupling effect.

The finite element method is selected to analyze the dynamic response in this paper. The keystone of the research is not the mechanism of fracture failure but the influence of cable dropping on the dynamic response of a tower-conductor coupling system.

Cable or insulator rupture is simulated by the following three steps:

1) Initial static equilibrium configuration of a tower-conductor coupling system is calculated.

2) Cable or insulator rupture is modeled by using the element death option[7].

3) Dynamic response of the coupling system is analyzed for the cable dropping process. Under the condition of cable rupture, the contact between the cable and the earth is temporarily not considered.

The self-weight application is performed in 10 load increments, and the static load(gravity action) is then maintained until a fictitious time $t = 10$ s. Then, the element death option is activated for the dynamic analysis at time 10 s + t. The calculation time interval t is 0.01 s.

The transmission line system is a statically indeterminate structure with finite degrees of freedom, so the finite element method is used to analyze the dynamic response of the tower-conductor coupling system. Equations of motion of a nonlinear multiple degrees-of-freedom system subjected to shock loads are solved by using a direct integration method.

The three-dimensional displacement of each member can be represented by

$$\left.\begin{aligned} u_1(x,y,z,t) &= \sum_{i=1}^{n} N_i(x,y,z)\,u_{1i}(t) \\ u_2(x,y,z,t) &= \sum_{i=1}^{n} N_i(x,y,z)\,u_{2i}(t) \\ u_3(x,y,z,t) &= \sum_{i=1}^{n} N_i(x,y,z)\,u_{3i}(t) \end{aligned}\right\} \tag{1}$$

where x, y, z are the coordinates of an element node, and N_i is the corresponding interpolation function.

Equations of three-dimensional elastodynamics are introduced as follows:

$$\sigma_{ij,j} + f_i - \rho u_{i,tt} - \mu u_{i,t} = 0 \tag{2}$$

$$\sigma_{ij} = D_{ijkl}\varepsilon_{kl} \tag{3}$$

$$\sigma_{ij} n_j = \overline{T_i} \tag{4}$$

where balance equation, physical equation and boundary condition of force are expressed by Eqs. (2), (3) and (4), respectively. $\sigma_{ij,j}$ is the partial derivative of the stress tensor based on independent coordinate x_j. ρ is the mass density, and μ is the damping coefficient. $u_{i,tt}$ and $u_{i,t}$ are the second and the first derivatives of u_i based on t. The proportional factor D_{ijkl} is an elastic constant. $\overline{T_i}$ represents the boundary condition of the transmission line system.

Equivalent integral form of Eqs. (2) and (4) with Galerkin methods can be expressed as

$$\begin{aligned} &\int_V \delta u_i(\sigma_{ij,j} + f_i - \rho u_{i,tt} - \mu u_{i,t})\,\mathrm{d}V - \\ &\int_{S_\sigma} \delta u_i(\sigma_{ij} n_j - \overline{T}_i)\,\mathrm{d}s = 0 \end{aligned} \tag{5}$$

The first term $\int_V \delta u_i \sigma_{ij,j}\,\mathrm{d}V$ in Eq. (5) is integrated by using integration by parts, and then substituted into Eq. (3). We can obtain

$$\begin{aligned} &\int_V (\delta\varepsilon_{ij} D_{ijkl}\varepsilon_{kl} + \delta u_i \rho u_{i,t} + \delta u_i \mu u_{i,t})\,\mathrm{d}V = \\ &\int_V \delta u_i f_i \mathrm{d}V + \int_{S_\sigma} \delta u_i \overline{T}_i \mathrm{d}s \end{aligned} \tag{6}$$

After Eq. (1) is substituted into Eq. (6), the solving equation of the coupling system is achieved as follows:

$$\boldsymbol{M}\ddot{\boldsymbol{u}}(t) + \boldsymbol{C}\dot{\boldsymbol{u}}(t) + \boldsymbol{K}\boldsymbol{u}(t) = \boldsymbol{Q}(t) \tag{7}$$

where $\ddot{\boldsymbol{u}}(t)$ and $\dot{\boldsymbol{u}}(t)$ are the acceleration and velocity vectors of the coupling system, respectively; $\boldsymbol{M}, \boldsymbol{C}, \boldsymbol{K}$ and $\boldsymbol{Q}(t)$ are the mass matrix, damping matrix, stiffness matrix and load vector, respectively.

The displacement, velocity and acceleration of the coupling system are represented by $\boldsymbol{u}_0$, $\dot{\boldsymbol{u}}_0$ and $\ddot{\boldsymbol{u}}_0$. Provided that the time domain is divided into n time intervals, the solution at time $t + \Delta t$ is the aim of the calculation when the solutions of time 0, Δt, $2\Delta t$, …, t have been known. In the time domain, the equations are defined as

$$\dot{\boldsymbol{u}}_{t+\Delta t} = \dot{\boldsymbol{u}}_t + [(1-\delta)\ddot{\boldsymbol{u}}_t + \delta\ddot{\boldsymbol{u}}_{t+\Delta t}]\Delta t \tag{8}$$

$$\boldsymbol{u}_{t+\Delta t} = \boldsymbol{u}_t + \dot{\boldsymbol{u}}_t\Delta t + \left[\left(\frac{1}{2} - \alpha\right)\ddot{\boldsymbol{u}}_t + \alpha\ddot{\boldsymbol{u}}_{t+\Delta t}\right]\Delta t^2 \tag{9}$$

where α and θ are the calculation parameters based on integral precision and stability. The unconditional stability integration scheme is introduced with $\alpha = 0.25$ and $\theta = 0.5$.

By solving Eq. (9), we obtain

$$\ddot{\boldsymbol{u}}_{t+\Delta t} = \frac{1}{\alpha\Delta t^2}(\boldsymbol{u}_{t+\Delta t} - \boldsymbol{u}_t) - \frac{1}{\alpha\Delta t}\dot{\boldsymbol{u}}_t - \left(\frac{1}{2\alpha} - 1\right)\ddot{\boldsymbol{u}}_t \tag{10}$$

Then, Eq. (10) is introduced into Eq. (8), and a new equation is substituted into Eq. (7). The two-step recursive formula is obtained as follows:

$$\left(\boldsymbol{K}+\frac{1}{\alpha\Delta t^2}\boldsymbol{M}+\frac{\delta}{\alpha\Delta t}\boldsymbol{C}\right)\boldsymbol{u}_{t+\Delta t}=\boldsymbol{Q}_{t+\Delta t}+\boldsymbol{M}\left[\frac{1}{\alpha\Delta t^2}\boldsymbol{u}_t+\frac{1}{\alpha\Delta t}\dot{\boldsymbol{u}}_t+\left(\frac{1}{2\alpha}-1\right)\ddot{\boldsymbol{u}}_t\right]+\boldsymbol{C}\left[\frac{\delta}{\alpha\Delta t}\boldsymbol{u}_t+\left(\frac{\delta}{\alpha}-1\right)\dot{\boldsymbol{u}}_t+\left(\frac{\delta}{2\alpha}-1\right)\Delta t\ddot{\boldsymbol{u}}_t\right] \tag{11}$$

$\boldsymbol{u}_t$ can be achieved by solving Eq. (7), and then introduced into the corresponding geometric and physical equation to obtain the dynamic response of the coupling system.

3 Case Study

A domestic double-circuit 500-kV high-voltage transmission line section is taken as a case to study the dynamic response under cable or insulator rupture. A self-erecting two-circuit steel tower is used. There are two groups of ground wires attached to the ground support, and the insulator with a length of 1 m is used to connect the ground wire and ground support. There are two groups of conductors attached to the cross arm, and the insulator with a length of 4 m is used to connect the conductor and the cross arm.

3.1 Line data

In order to make the analysis tractable, it is assumed that the towers of the same drum type are chosen in the line section. The height of the tower is 54.3 m. The span distance between two adjacent towers is 400 m. The components of the tower are made of Q345 and Q235 angle steel, so the elastic modulus and the mass density of the components of the tower are 206 GPa and 7.8×10^3 kg/m^3, respectively.

The conductors are LGJ-400/35 steel cored aluminium stranded wire. The material forming the inner core strands is galvanized steel, whereas the outer strands are aluminum. The shield wire is an aluminium-clad wire strands wire. Calculation parameters of the conductor are listed in Tab. 1.

Tab. 1 Calculation parameters of the conductor and ground wire

Type	Area/mm^2	Modulus of elasticity/GPa	Mass per unit length/(kg · m^{-1})	Initial horizontal tension/kN
Conductor	425.24	65	1.349	19.2
Ground wire	152.81	178	0.675	11.6

3.2 FE model

According to the calculation hypothesis and the modeling approach, the three-dimensional elaborate FE model of a strain section is established and shown in Fig. 1. The strain section includes four steel suspension towers of the same height and altitude, and the locations of the towers are on the same straight line. The initial equilibrium condition of the coupling system model is verified by form finding analysis. The conductor and ground wire tension at the lowest point of one span transmission line in static results is approximate to that in the design parameters in Tab. 2.

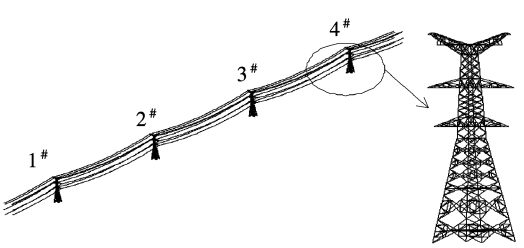

Fig. 1 Baseline model of transmission lines

Tab. 2 Design parameters of the conductor and ground wire

Type	Calculated breaking force/kN	Maximum suitable force/kN	Average operation force/kN
LGJ-400/35 (conductor)	98.705	39.482	24.676
JL/LB1A-95/55 (ground wire)	79.230	26.410	11.885

3.3 Results

The vertical displacement (Z displacement) of failure point is analyzed. The axial force of the conductor at suspension points, the insulator, and the component of the upper cross arm next to the failure point are computed and saved. The calculation points of the tower-conductor coupling system are shown in Fig. 2.

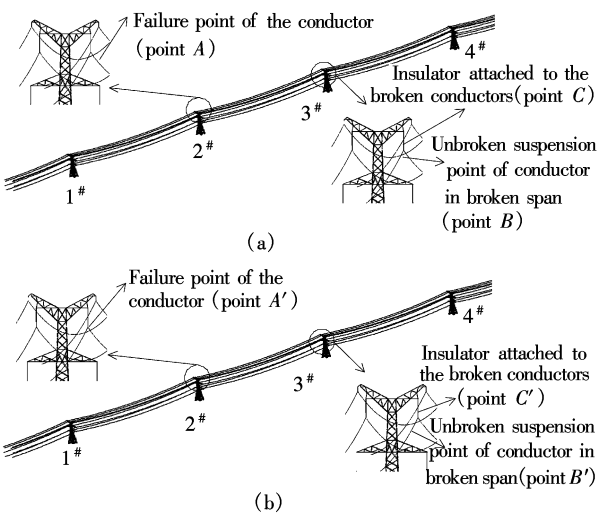

Fig. 2 Calculation points. (a) Cable rupture; (b) Insulator rupture

In order to compare the dynamic response between cable and insulator rupture, the dynamic effect coefficient η and the dynamic magnification factor ρ, which are defined according to Eqs. (12) and (13), are introduced here.

$$\eta=\frac{P_{\text{peak}}}{P_{\text{static}}} \tag{12}$$

$$\rho=\frac{P_{\text{peak}}}{P_{\text{steady}}} \tag{13}$$

where P_{peak} is the maximum axial force of the structural element in the dropping process; P_{static} is the static axial force of the structural element, and P_{steady} represents the axial tension of the structural element at the end of the dropping process.

3.3.1 Movement of the conductor

The motion of the transmission line system, which is not

a linear process, can be considered as a superposition of rigid motion and elastic motion. The vertical displacements of points A and A' in Fig. 2 are shown in Fig. 3.

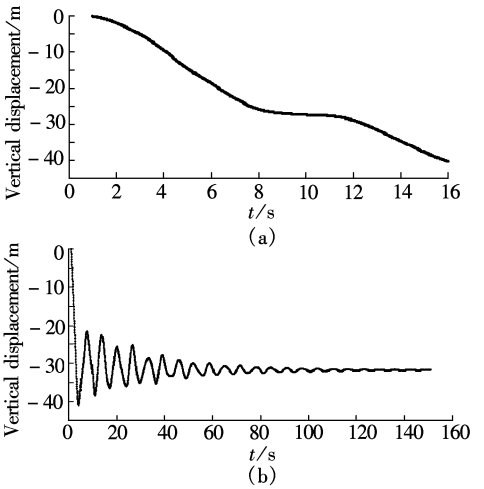

Fig. 3 Vertical displacements of rupture points. (a) Cable rupture; (b) Insulator rupture

According to Fig. 3(a), the vertical displacement of point A decreases all the time during the cable dropping process.

Fig. 3(b) shows the motion track of breaking point A'. The obvious rebound phenomenon occurs in the dropping process of cables, and the maximum resilience value is 20 m.

3.3.2 Axial force of the conductor

In order to analyze the influence of fracture failure on other conductors adjacent to the broken point, the conductor tension of the broken span (points B and B' in Fig. 2) is computed.

Under cable rupture, the dynamic tension in the conductor decreases in the cable dropping process, as shown in Fig. 4(a).

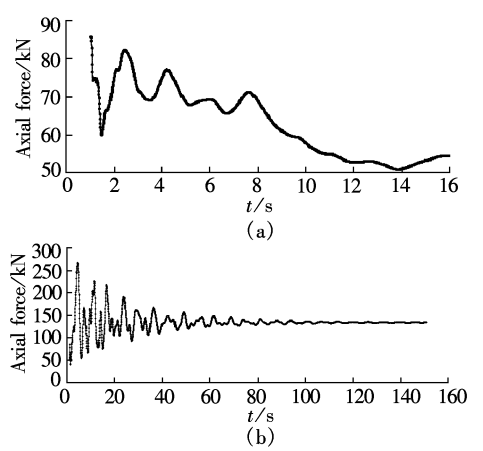

Fig. 4 Axial force of the conductor adjacent to failure span. (a) Cable rupture; (b) Insulator rupture

Under insulator rupture, Fig. 4(b) shows the dynamic tension in the conductors during the cable dropping process. The dynamic tension increases rapidly, then slowly decreases, and finally reaches a stable value. η and ρ are 3 and 1.97, respectively. In the technical code for designing a 110 to 500 kV overhead transmission line, the value of the calculation breaking force at the suspension point of the transmission line is defined within 66% of the design value of the calculation breaking force in the case of rare wind speed or icing. According to Tab. 2, the design value of the calculation breaking force is 98.705 kN. The calculated peak tension at the suspension point of the transmission line is 65.439 kN which exceeds 66% of the design value of the calculation breaking force.

3.3.3 Axial force of the insulator

The insulator is a key element which is used to connect the tower and the conductors. The dynamic response of the insulator has some influence on the internal force distribution of the tower-conductor coupling system. The conductor tension of the insulator (points C and C' in Fig. 2) is computed.

It can be seen in Fig. 5(a) that the insulator tension trends to increase nonlinearly under cable rupture. The static insulator tension is 13 kN, which increases to 19 kN before the conductor collides with the ground.

As seen in Fig. 5(b), the insulator tension under insulator rupture increases rapidly, then slowly decreases, and finally reaches a stable value. η and ρ are 4.8 and 2.6, respectively.

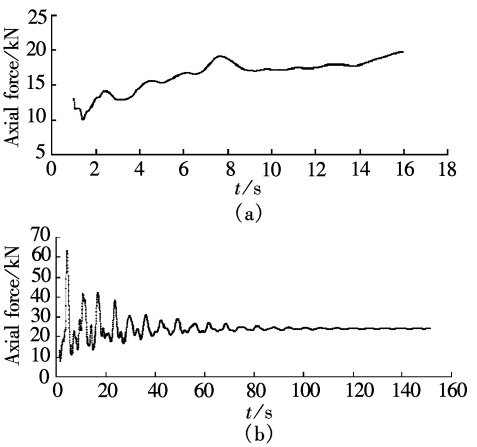

Fig. 5 Axial force of the insulator adjacent to failure span. (a) Cable rupture; (b) Insulator rupture

In a word, cable and insulator rupture both affect the dynamic force of the insulator attached to the broken conductors.

3.3.4 Axial force of the cross arm

To study a line section subjected to cable or insulator breakage is similar to study the propagation of a shock wave in a highly nonlinear system. The shock wave induced by cable dropping is transmitted to the cross arm of the tower through the insulator. The cross arm is the critical position of the tower (see Fig. 6).

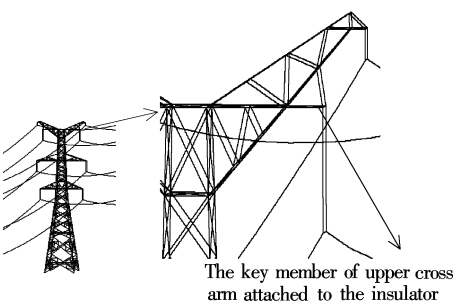

Fig. 6 Calculation point of upper crossarm

According to Fig. 7(a), the tension in the upper cross arm trends to increase nonlinearly under cable rupture and η is 1.4.

As seen in Fig. 7(b), the dynamic tension of the upper cross arm under insulator rupture increases rapidly, then slowly decreases, and finally reaches a stable value. η and ρ are 1.5 and 1.73, respectively.

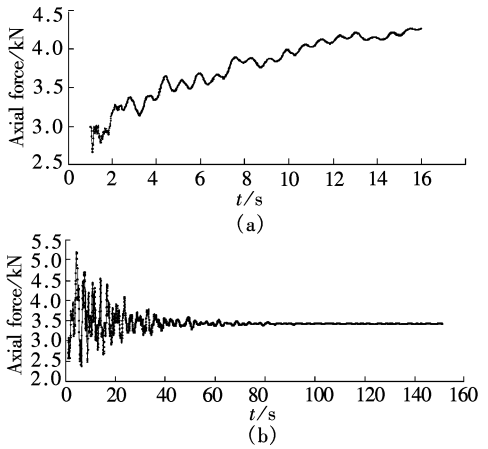

Fig. 7 Axial force of upper crossarm. (a) Cable rupture; (b) Insulator rupture

4 Conclusions

1) Under cable rupture, upper crossarm cable rupture has no effect on cable tension at adjacent suspension points, but it has a significant influence on tension in the insulator and the tower component of the upper crossarm next to the broken span.

2) Under insulator rupture, the peak tension in the conductor of the upper crossarm at suspension point exceeds the design value. Insulator rupture has little effect on the tower component of the upper crossarm, but it has a great influence on the insulator tension of the upper crossarm.

3) It is unreasonable to consider only line breaking load in the technical code for designing a 110 to 500 kV overhead transmission line in China, and insulator rupture conditions should be considered in the design value for tower and pole structures of overhead transmission lines.

4) Nonlinear dynamic response should be considered in the design, and the static calculation mode in the analysis of conductor breaking tension and longitudinal unbalanced conductor tension is unreliable.

References

[1] East China Electric Power Design Institute. DL/T 5092—1999 Technical code for designing 110-500 kV overhead transmission line [S]. Beijing: China Electric Power Press, 1999. (in Chinese)

[2] Southwest Electric Power Design Institute. DL/T 5154—2002 Technical regulation of design for tower and pole structures of overhead transmission line [S]. Beijing: China Electric Power Press, 2002. (in Chinese)

[3] Siddiqui F M A. Dynamic analysis and behavior of electric transmission line systems subjected to broken wires [D]. Pittsburgh: Department of Engineering of University of Pittsburgh, 1981.

[4] Baenziger M. Broken conductor loads on transmission line structures [D]. Madison: University of Wisconsin-Madison, 1981.

[5] Thomas M B, Peyrot A H. Dynamic response of ruptured conductors in transmission lines [J]. *IEEE Transactions on Power Apparatus Systems*, 1982, **PAS-101**(9): 3022 − 3027.

[6] McClure G, Tinawi R. Mathematical modeling of the transient response of electric transmission lines due to conductor breakage [J]. *Computers and Structures*, 1987, **26**(1/2): 41 − 56.

[7] McClure G, Lapointe M. Modeling the structural dynamic response of overhead transmission lines [J]. *Computers and Structures*, 2003, **81**(8): 825 − 834.

[8] Vincent Pierre, Huet Claude, Charbonneau Marc, et al. Testing and numerical simulation of overhead transmission line dynamics under component failure conditions [C]//*Proceedings of the* 40*th General Session of CIGRE*. Paris, 2004: B2-308.

[9] Shimo Yoji. Development of power transmission line inspection system by unmanned helicopter [C]//*Proceedings of the* 41*st General Session of CIGRE*. Paris, 2006: B2/D2-106.

[10] Clark M, Richards D J, Clutterbuck D, et al. Measured dynamic performance of electricity transmission towers following controlled broken-wire events [C]//*Proceedings of the* 41*st General Session of CIGRE*. Paris, 2006: B2-313.

[11] Chen Yi. Wind-induced response and vibration control of long span transmission line system [D]. Shanghai: School of Civil Engineering of Tongji University, 2003. (in Chinese)

高压输电线路导线跌落非线性动响应分析

夏开全[1] 刘 云[2] 钱振东[2]

([1] 中国电力科学研究院,北京 100055)

([2] 东南大学智能运输系统研究中心,南京 210096)

摘要: 为了研究机械性故障对高压输电线路耦合体系的受力影响,建立了输电线路耐张段的非线性耦合体系模型,通过导线找形非线性静力计算确定了耐张段的初始平衡状态.采用瞬态动力分析方法计算了导线、绝缘子破坏失效危险工况下的输电线路耦合体系非线性动响应.分析结果表明,上横担一组导线断裂失效对邻近端导线张力没有明显影响,对邻近端的绝缘子及铁塔横担构件的受力有较大的影响;上横担一组绝缘子破坏失效后,破坏档未破坏端导线的张力超过了技术规程中的设计值;导线的跌落对破坏档未破坏端的上横担绝缘子受力有较大的影响,而对上横担铁塔杆件没有明显的影响;在架空送电线路的设计中应该考虑绝缘子断裂的荷载工况.研究成果可为输电线路结构设计提供理论依据.

关键词: 高压输电线路;瞬态响应;导线跌落;数值模拟;有限单元法

中图分类号: TM753